

Mechanism for enhancement of electrical activation of silicon in GaAs by aluminum co-implantation

J. P. de Souza and D. K. Sadana

Citation: [Applied Physics Letters](#) **63**, 3200 (1993); doi: 10.1063/1.110198

View online: <http://dx.doi.org/10.1063/1.110198>

View Table of Contents: <http://scitation.aip.org/content/aip/journal/apl/63/23?ver=pdfcov>

Published by the [AIP Publishing](#)

Articles you may be interested in

[Electrical behavior of implanted carbon impurities in fluorine co-implanted GaAs](#)

J. Appl. Phys. **80**, 3834 (1996); 10.1063/1.363337

[Complete p-type activation in vertical-gradient freeze GaAs co-implanted with gallium and carbon](#)

Appl. Phys. Lett. **68**, 1537 (1996); 10.1063/1.115691

[The effect of coimplantation on the electrical activity of implanted carbon in GaAs](#)

J. Appl. Phys. **74**, 7118 (1993); 10.1063/1.355027

[High activation efficiency in Mg⁺ implanted GaAs by P⁺ coimplantation](#)

Appl. Phys. Lett. **61**, 2093 (1992); 10.1063/1.108317

[Activation efficiency improvement in Si-implanted GaAs by P co-implantation](#)

Appl. Phys. Lett. **50**, 1592 (1987); 10.1063/1.97790

The advertisement features a blue and orange background with a molecular structure graphic. On the left is a thumbnail of an 'Applied Physics Reviews' journal cover showing a diagram of a device. The main text reads 'NEW Special Topic Sections' in large white letters. Below this, it says 'NOW ONLINE' in yellow, followed by 'Lithium Niobate Properties and Applications: Reviews of Emerging Trends' in white. The AIP Applied Physics Reviews logo is in the bottom right corner.

NEW Special Topic Sections

NOW ONLINE
Lithium Niobate Properties and Applications:
Reviews of Emerging Trends

AIP Applied Physics Reviews

Mechanism for enhancement of electrical activation of silicon in GaAs by aluminum co-implantation

J. P. de Souza

Instituto de Física, UFRGS, 91501-970 Porto Alegre, R.S., Brazil

D. K. Sadana

Thomas J. Watson Research Center, IBM, Yorktown Heights, New York 10598

(Received 2 June 1993; accepted for publication 24 September 1993)

A pronounced enhancement in the electrical activation of implanted Si in GaAs is demonstrated by co-implantation of Al. The maximum enhancement ($\times 2$) occurs when the Si distribution is shallow, there is a separation between the Si and Al distributions with the Al being deeper, the Si and Al are implanted at doses of $< 1 \times 10^{13} \text{ cm}^{-2}$, and subsequent annealing of the co-implanted GaAs is performed under capless or proximity cap conditions. A model considering gettering of the oxygen present in the bulk Czochralski-grown GaAs to the implanted Al is invoked to explain the observed activation enhancement.

Only a fraction of implanted n dopants is electrically active in GaAs even after the most optimized annealing.¹ Co-implantation of n dopants which occupy Ga sites (e.g., Si) with a column V element (e.g., P) and those which occupy As sites with column III impurity (e.g., Ga) has been reported to enhance the dopant activation in GaAs.²⁻⁸ It was previously shown that Al co-implantation with n dopants followed by capless rapid thermal annealing (RTA) enhances the electrical activation of these dopants in GaAs.⁹ The maximum carrier enhancement due to Al co-implantation occurs at n -dopant doses typically used for n channels in GaAs metal-semiconductor field-effect-transistors (MESFETs) (i.e., $< 1 \times 10^{13} \text{ cm}^{-2}$).

The effect of Al co-implantation (at 160 keV) on the Si activation and on Hall mobility in the Al dose range of 1.5×10^{11} – $4.5 \times 10^{13} \text{ cm}^{-2}$ has been discussed earlier.⁹ The Si activation increases initially with the Al dose and the maximum carrier enhancement occurs at an Al dose of $4.5 \times 10^{12} \text{ cm}^{-2}$. The Si activation and carrier mobility begin to deteriorate at higher Al doses. At an Al dose of $4.5 \times 10^{13} \text{ cm}^{-2}$ the Si was mostly deactivated, which is in agreement with the published data of Farley and Streetman.⁶

In this letter the activation enhancement of implanted Si has been studied systematically as a function of Al⁺ energy. Due to lack of space the electrical data from only those Al doses is included which resulted in the maximum carrier enhancement. It is shown that the position of the Al profile with respect to the implanted Si profile determines where the electrical activation enhancement occurs spatially in the Si implanted region. Control experiments with dual Al and O implant indicate that Al can strongly getter oxygen present in the implanted GaAs substrate. The role of oxygen gettering in electrical activation enhancement is further confirmed with a Mg co-implant since like Al, Mg also has a strong bond with O. A phenomenological model which explains the observed activation behavior is proposed.

Semi-insulating CZ grown LEC (100) GaAs wafers were either implanted with $^{29}\text{Si}^+$ only (30 keV, $6.0 \times 10^{12} \text{ cm}^{-2}$) (control sample) or were dual implanted with Al⁺

at energies of 30 (sample A), 160 (sample B), and 450 keV (sample C) with doses of 1.5 , 4.5 , and $10 \times 10^{12} \text{ cm}^{-2}$, respectively.

The implanted wafers subsequently underwent RTA with either a Si-proximity cap or with a conventional plasma enhanced chemical vapor deposited (PECVD) Si_xN_y cap. The Si-proximity RTA will be referred to as capless RTA from here on in the text. The electrical characterization of the annealed samples was performed by CV and Hall measurements. Atomic profiles of Si, Al, and O on a selected number of samples were obtained by secondary ion mass spectrometry (SIMS).

Figure 1 shows atomic profiles of Si and Al from samples B and C after capless RTA at 850°C for 10 s (the as-implanted and annealed profiles of Al and Si were indistinguishable from each other).

Carrier concentration profiles (CV) of the control sample and those of samples C after capless RTA at $850^\circ\text{C}/10 \text{ s}$ are shown in Fig. 2 [curves (i)–(iv)], respectively. In sample A where the Al and Si depth profile are spatially coincident the Si activation is enhanced primarily in the tail region [compare curves (i) and (ii)]. However, the Si activation remains practically unaffected in the peak region in sample A. When the Al profiles were deeper than

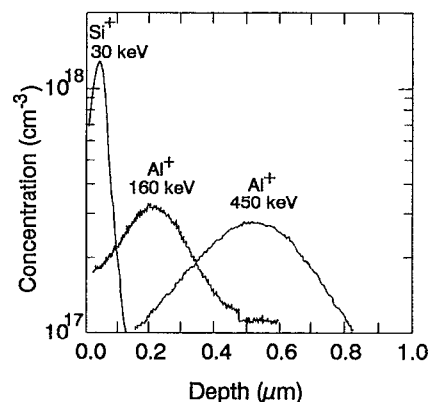


FIG. 1. Atomic profiles (SIMS) of implanted ^{29}Si and Al from samples B and C after capless annealing at 850°C for 10 s.

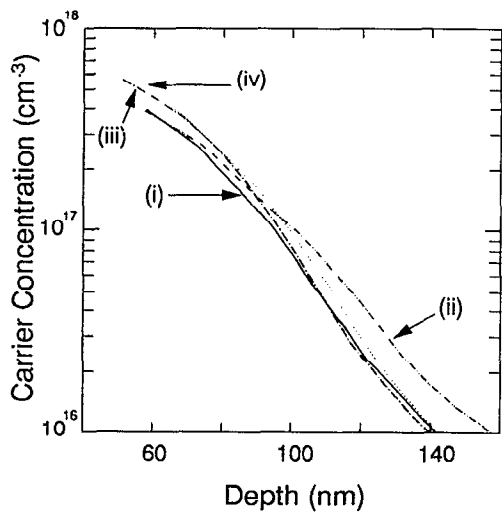


FIG. 2. Carrier concentration profiles (CV) from the sample implanted only with Si [control sample, curve (i)], from the sample co-implanted with Al profiles matching Si and [sample A, curve (ii)], from the samples co-implanted with Al at 160 keV [sample B, curve (iii)] and at 450 keV [sample C, curve (iv)]. The samples were capless annealed at 850 °C for 10 s.

the Si profile (samples B and C) a pronounced enhancement in the carrier concentration occurred in the near-surface region ($<0.1 \mu\text{m}$). In the tail region, however, there is no measurable enhancement [compare curves (iii) and (iv) with curve (i) in Fig. 2].

The effect of a PECVD Si_xN_y cap on the electrical activation of the co-implanted samples was drastic. In contrast to the pronounced activation enhancement after capless anneal, a pronounced reduction ($\times 3$ – $\times 4$) occurred in the carrier density of sample B after capped RTA at 850 °C/10 s. The Si activation continued to deteriorate as the annealing time was increased for the capped sample. For example, furnace annealing of capped samples at 840 °C for 20 min converted the samples from n to p -type with sheet carrier densities down to $<9 \times 10^{11} \text{ cm}^{-2}$.

To explain the carrier enhancement in Fig. 2 we propose a model which invokes gettering of the oxygen in the starting GaAs substrate by the co-implanted Al during the activation anneal. Depending on the manufacturer, the oxygen content in a CZ-grown GaAs can be up to $2 \times 10^{17} \text{ cm}^{-3}$. It is believed that the oxygen gettering occurs due to its strong chemical affinity for Al. The oxygen migration towards the implanted Al is probably facilitated by the cumulative damage created by the dopant and Al implants. Since O is known to act as a deep double electron trap and compensates n dopants in GaAs,¹⁰ the depletion of O atoms in the n -dopant implanted region should enhance the dopant activation. In addition, the O gettering should liberate the dopants from dopant-O complexes and this should further enhance the dopant activation.

In order to determine whether Al-O gettering can indeed occur in GaAs the following control experiment was conducted. $^{18}\text{O}^+$ and Al^+ were co-implanted with a dose of $1.0 \times 10^{13} \text{ cm}^{-2}$ each at energies of 67 and 200 keV, respectively, into the GaAs substrates obtained from the same boule as those used for dopant implants. The energies

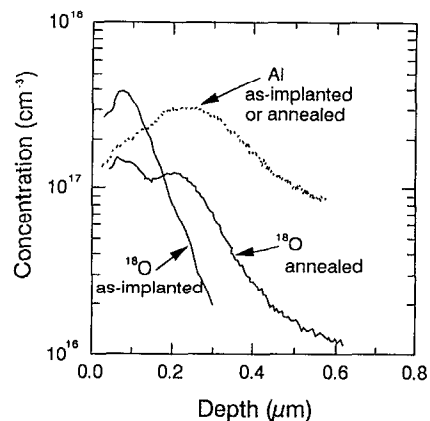


FIG. 3. Atomic profiles (SIMS) of implanted ^{18}O ($1.0 \times 10^{13} \text{ cm}^{-2}$ at 67 keV) and of Al ($1.0 \times 10^{13} \text{ cm}^{-2}$ at 200 keV) before and after capless RTA at 850 °C for 10 s.

of Al^+ and O^+ were chosen to obtain a spatial separation between these elements so that their redistributions after the annealing could be observed. The samples subsequently underwent capless RTA at 850 °C/10 s. The ^{18}O isotope was used to improve SIMS sensitivity for oxygen detection. A pronounced redistribution of the ^{18}O in the Al/O co-implanted sample occurs after RTA (Fig. 3). The initial nearly Gaussian distribution of as-implanted ^{18}O converts into a bimodal distribution after the RTA. The Al does not show any significant redistribution during the RTA. The first peak of ^{18}O is located approximately at a depth corresponding to the mean projected range of the ^{18}O implanted profile and the second one located in the Al implanted region. These data (Fig. 3) clearly support the O gettering theory. The effect of the Al is expected to be most pronounced at doses where the proportion of the background ($<1 \times 10^{17} \text{ cm}^{-3}$) oxygen relative to implanted dose is significant, i.e., in the low dose regime ($<1 \times 10^{13} \text{ cm}^{-2}$).

In order to further test the O gettering model additional experiments where Al was replaced by Mg were conducted. It should be noted that the Mg–O bond (3.4 eV)¹¹ is almost as strong as the Al–O bond (5.0 eV).¹¹ The Mg^+ implanted sample ($1.5 \times 10^{12} \text{ cm}^{-2}$ at 160 keV) was submitted to a capless RTA at 850 °C/10 s prior to the Si implantation. After the Si^+ implantation a second capless RTA at 850 °C/10 s was performed in the co-implanted sample. Figure 4 shows carrier profiles of the control and Mg co-implanted samples. Since Mg is a p -type dopant it creates a buried p layer in GaAs, which explains the observed compensation in the tail region. However, the enhancement of in the Si activation in the near-surface region is consistent with the oxygen gettering model proposed above.

Now we explain the spatial dependence of the Si activation on the Al^+ energy. If it is assumed that O tracks the Al, the tail region of the Si profile will have reduced the O concentration in sample A. Consequently, enhanced Si activation in the tail region is expected [Fig. 2, curve (ii)]. On the other hand, in samples B and C where the Al

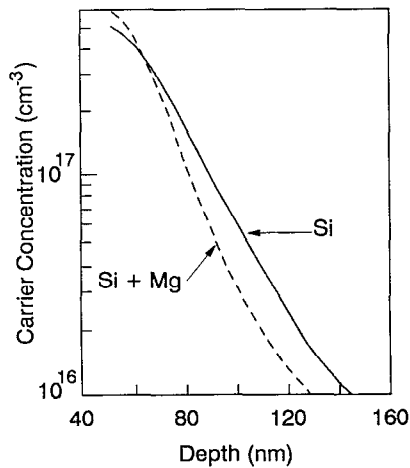


FIG. 4. Carrier concentration profiles (CV) from a sample implanted only with Si (control sample) and from a sample co-implanted with Mg ($1.5 \times 10^{12} \text{ cm}^{-2}$ at 160 keV) after capless RTA at 850 °C for 10 s.

profiles are deep the O is gettered away from the peak region of the Si profile, resulting in higher electrical activation there.

It is believed that the deterioration of the Si activation in the capped annealed samples is related to the H diffusion from the cap during the anneal.¹² Perhaps the H from the

cap decreases the O gettering efficiency of the Al due to Al—H interaction.

It is conceivable that point defects are also playing an important role in determining the Si activation in co-implanted samples. However, the observed activation enhancement can be directly correlated with the O movement.

¹ S. J. Pearton, *Solid State Phenom.* **1&2**, 247 (1988).
² B. J. Sealy, E. C. Bell, R. K. Surridge, K. G. Stephens, T. Ambridge, and R. Heckingbottom, *Inst. Phys. Conf. Ser.* **28**, 75 (1976).
³ T. Inada, S. Kato, T. Ohkubo, and T. Hara, *Radiat. Eff.* **48**, 91 (1980).
⁴ Y. S. Park, Y. K. Yeo, and F. L. Pedrotti, *Nucl. Instrum. Methods* **182/183**, 617 (1981).
⁵ H. Kräutle, *Nucl. Instrum. Methods* **182/183**, 625 (1981).
⁶ C. W. Farley, T. S. Kim, and B. G. Streetman, *J. Electron. Mater.* **16**, 79 (1987).
⁷ F. Hyuga, H. Yamazaki, K. Watanabe, and J. Osaka, *Appl. Phys. Lett.* **50**, 1592 (1987).
⁸ G. Marrakchi, A. Laugier, G. Guillot, S. Alaya, and H. Maaref, *Appl. Phys. Lett.* **59**, 923 (1991).
⁹ J. P. de Souza and D. K. Sadana, in *Advanced III-V Compound Semiconductors Growth, Processing and Devices*, edited by S. J. Pearton, D. K. Sadana, and J. M. Zavada (Materials Research Society, Pittsburgh, 1992), Vol. 240, p. 887.
¹⁰ P. N. Favennec, *J. Appl. Phys.* **47**, 2532 (1976).
¹¹ C. T. Lynch, in *Materials Science: General Properties* (CRC, Cleveland, OH, 1974), p. 76.
¹² J. P. de Souza, D. K. Sadana, H. Baratte, and F. Cardone, *Appl. Phys. Lett.* **57**, 1129 (1990).